Available online at www.sciencedirect.com

SciVerse ScienceDirect

Ceramics International 39 (2013) 1957–1962

CERAMICS INTERNATIONAL

www.elsevier.com/locate/ceramint

Synthesis of SiC nanowires by thermal evaporation method without catalyst assistant

Kai Chen, Zhaohui Huang*, Juntong Huang, Minghao Fang, Yan-gai Liu, Haipeng Ji, Li Yin

School of Materials Science and Technology, China University of Geosciences (Beijing), Xueyuan Road, Beijing 100083, China

Received 11 June 2012; received in revised form 14 August 2012; accepted 15 August 2012
Available online 23 August 2012

Abstract

In this paper, SiC nanowires were successfully synthesized on Si substrate by the thermal evaporation method without the assistance of a metal catalyst. The phase composition, morphology and microstructure of the SiC–SiO_2 core–shell nanowires were investigated by X-ray diffraction (XRD), field emission scanning electron microscopy (FESEM), energy dispersive spectroscopy (EDS), transmission electron microscopy (TEM), and high-resolution transmission electron microscopy (HRTEM). The SiC nanowires produced grew along the [111] direction and had diameters of 50–100 nm with lengths of several hundreds of microns. The SiC nanowire was composed of a single-crystalline SiC core with a thin amorphous SiO_2 shell. The growth mechanism of the nanowires can be explained by the vapor–solid (VS) process.

Keywords: D. SiC; Nanowires; Vapor–solid process; SiC–SiO_2 core–shell structure

1. Introduction

Since the discovery of carbon nanotubes, one-dimensional (1D) nanostructures, particularly nanowires, have become the focus of intensive research due to their unique mechanical, physical, chemical, optical, and electrical properties with respect to the corresponding bulk materials [1–5]. Silicon carbide (SiC) being an important wide band gap semiconductor, SiC nanowires exhibit many excellent electronic, physical, and chemical properties rendering them suitable for many harsh conditions, including high temperature, high thermal conductivity, high power, and high frequency [1,6]. The outstanding mechanical properties of SiC nanowire make it a promising candidate for the reinforcing phase in ceramic, metal, and polymer matrix composites. SiC nanowires also show potential for fruitful applications in field emission displays, nanosensors, nanoscale electro-devices and optoelectronic devices [7,8].

To date, much effort has been devoted to synthesizing SiC nanowires and a number of techniques have been developed, such as sol–gel combined carbothermal reduction [9,10], carbon nanotubes confined reaction [11,12], metal-assisted vapor–liquid–solid (VLS) mechanism [13,14], chemical vapor deposition (CVD) technology [15,16], high-frequency induction heating technology [17], polymeric precursor pyrolysis [18,19] and thermal evaporation method [20,21]. Most of these reported synthesis methods, however, involved complicated equipment and processes, which limit their further application and act as a barrier to further research and development in many fields. Furthermore, the resident metal catalyst used in these techniques, i.e., the sol–gel combined carbothermal reduction method, metal-assisted VLS growth mechanism and CVD technology, is very difficult to be removed after the synthesis process. Thus, a simpler and more effective method needs to be developed to prepare SiC nanowires.

In this paper, scales of SiC nanowires were successfully synthesized on Si (100) wafer by the thermal evaporation method without the assistance of a metal catalyst. The

*Corresponding author. Tel./fax: +86 10 82322186.
E-mail address: huang118@cugb.edu.cn (Z. Huang).

0272-8842/$ - see front matter © 2012 Elsevier Ltd and Techna Group S.r.l. All rights reserved.
http://dx.doi.org/10.1016/j.ceramint.2012.08.046

morphology, phase composition, and microstructure of the SiC nanowires were then characterized. A growth mechanism for these SiC nanowires and the synthesis process of the SiC–SiO_2 core–shell structure were explained.

2. Experimental

2.1. Synthesis of SiC nanowires

A columnar graphite crucible (100 mm in diameter and 40 mm in height) was used as a reactor to produce the SiC nanowires. An N-type Si (100) wafer (4 Ω cm, Beijing Zhongkekenuo New Energy Technology Co., Ltd., China) of dimension 2 cm × 4 cm was used as the substrate. The surface of this Si substrate was ultrasonically cleaned with acetone and ethanol for 10 min, and then dried in air. Graphite powder (purity 99.9 wt%; 5 g) was placed at the center of the graphite crucible. The aforementioned Si substrate was then placed in the crucible with the graphite powder–substrate distance of 1 cm as shown in Fig. 1. The crucible was covered by a graphite plate, and the whole set-up was placed at the center of a vacuum furnace which was evacuated to 10 Pa by a rotary pump. Argon gas (purity 99.999%) was then introduced until the furnace pressure reached 0.12 MPa and the argon pressure was maintained throughout the whole experiment process. The furnace temperature was initially raised to 1000 °C at a heating rate of 10 °C/min, then heating continued at 3 °C/min to a temperature of 1500 °C which was maintained further for 3 h. After cooling to room temperature, a green colored layer was removed for further analysis on the surface of Si substrates.

2.2. Characterization of SiC nanowires

The phase composition of the synthesized samples was determined by X-ray diffraction (XRD; D8 Advance diffractometer, Germany), using Cu $K\alpha_1$ radiation ($\lambda = 1.5406$ Å) with a step of 0.02° (2θ) and a scanning rate of 4° min^{-1}. The microstructures of the samples were examined by field emission scanning electron microscopy (FESEM, JEOL JSM6700F, Japan), energy dispersive spectroscopy (EDS, INCA, Oxford Instrument, UK), transmission electron microscopy (TEM, JEOL JEM-2010, Japan, accelerating voltage 200 keV, 4k × 2.7k Gatan CCD camera) and high-resolution transmission electron microscopy, and selected area electron diffraction (HRTEM and SAED, JEM-2010, Japan). Samples for TEM observation were dispersed in absolute ethanol by ultrasonication (KQ-100DB) for 10 min, and a drop of the suspension containing the products was dropped onto a copper grid coated with an amorphous carbon supporting film and then dried in air.

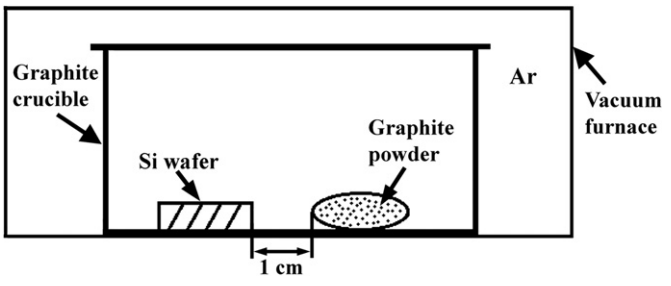

Fig. 1. Schematic diagram of experimental setup for the growth of SiC nanowires.

3. Results and discussion

3.1. XRD analysis

The XRD pattern of the SiC nanowires grown on the Si substrate is shown in Fig. 2. As can be seen from the pattern, three diffraction peaks indexed to (111), (200), and (220) were well matched with the standard face-centered cubic structure of 3C-SiC (JCPDS card No. 29-1129, $a = 4.359$ Å), which has the lattice constant of $a = 4.375$ Å. The strong intensities and narrow widths of the 3C-SiC peaks also indicated that the SiC nanowires were well-crystallized. Furthermore, the diffraction peak (111) was the only peak that gained a substantial increase independent of the intensity of the three 3C-SiC peaks. This indicated that the predominant growth orientation of the nanowires was along the (111) direction. In addition, the small diffraction peaks at 28.5° and 47.4° were due to the Si substrate.

3.2. FESEM analysis

Fig. 3 shows typical FESEM images of the synthesized SiC nanowires. The SEM image, as shown in Fig. 3(a), reveals the general morphology of nanowires. It can be seen clearly that both straight and curved nanowires grew randomly on the Si substrate at high density. The length of the nanowires was up to several hundreds of microns, and the diameters were uniformly about 50–100 nm. The length was similar to those of the SiC nanowires synthesized previously by other researchers [21–23]. Fig. 3(b) shows

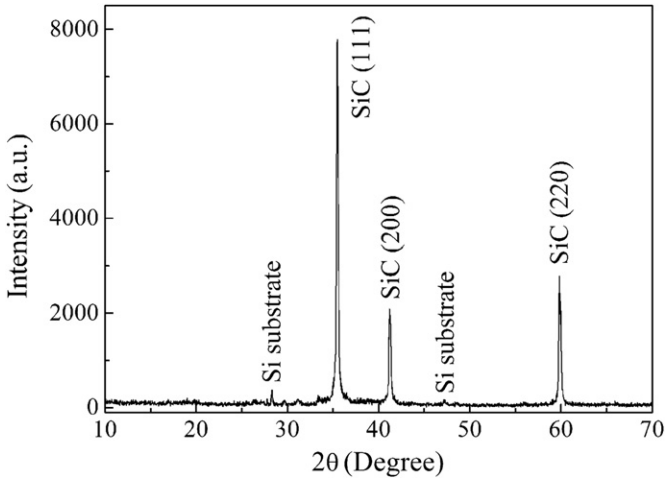

Fig. 2. XRD pattern of the as-obtained SiC nanowires.

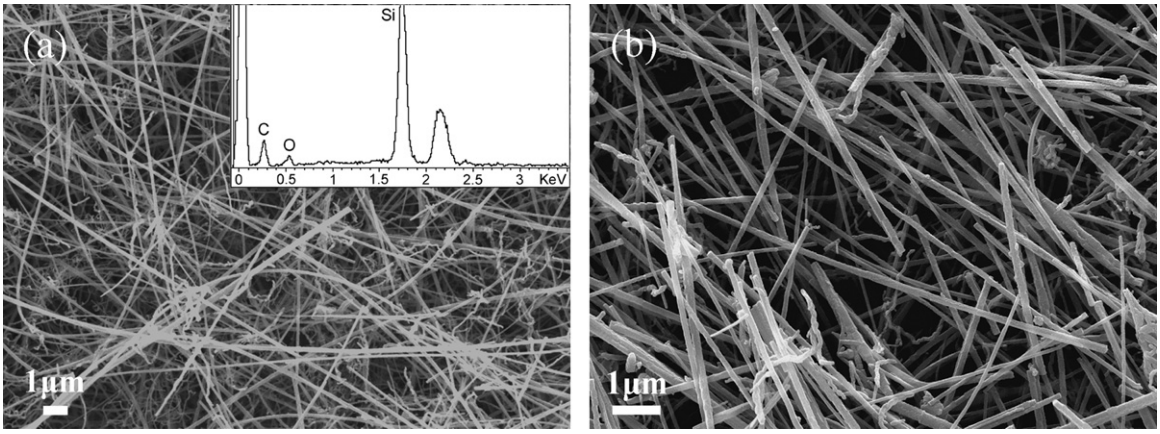

Fig. 3. (a) and (b) Typical low and high magnification FESEM images of SiC nanowires, respectively; inset in (a) is the corresponding EDS pattern.

that the nanowires with smooth surfaces were straight and randomly oriented, but no metal catalyst was found at the tips of the grown nanowires. The inset in Fig. 3(a) shows the EDS pattern of the as-obtained nanowires. The corresponding EDS analysis of the nanowires demonstrates that the product contained only C, Si, and O. Moreover, the atomic percentages of C, Si, and O were about 65.69%, 26.74%, and 7.56%, respectively. It is inferred that the SiC nanowires possessed a SiC–SiO_2 core–shell structure, which will be proved by TEM measurements in detail.

3.3. TEM analysis

The internal structure and crystallinity of synthesized SiC nanowires were characterized by TEM. Fig. 4(a) shows a typical TEM image of the SiC nanowires; it can be seen that no metallic balls were found at the tips of the nanowires. This indicates that the growth mechanism of SiC nanowires is not attributed to the VLS mechanism [14,16]. The high magnification TEM image, as shown in Fig. 4(b), reveals that the nanowire had a dark-contrasted crystal-core with a diameter of 50–80 nm, which was wrapped in a light amorphous layer shell with a thickness of 5–15 nm. HRTEM images of the core–shell heterostructure are given in Fig. 4(c) and (d). Akin to the aforementioned FESEM observation, it was confirmed that the core of nanowires was crystalline SiC and the shell was a thin amorphous SiO_2 layer. The SAED pattern of the nanowires reveals a crystalline structure (Fig. 4(d) inset). It can also be found that the crystalline nanowires typically possessed a high density of both stacking faults and planar defects. Fig. 4(c) and (d) also shows that the lattice fringes spacing of 0.25 nm corresponded to the (111) crystal plane spacing of 3C–SiC. The axis of the (111) crystal plane coincided with the longitudinal direction of SiC nanowires, which indicated that the nanowires grew along the [111] direction. This generally coincided with the largest planar spacing and the lowest specific surface energy of the (111) plane, thus providing further general evidence in support of the inference that the most favorable, preferred crystal growth orientation must have been along the [111] direction [12,13,22].

3.4. Growth mechanism of SiC nanowires

No catalyst was used during any stage of synthesis procedure. Thus, the growth mechanism in the thermal evaporation method of this study did not follow the previously reported VLS growth model [24]. Based on our experimental results, we believe that the vapor–solid (VS) process was the main growth mechanism for the SiC nanowires. The FESEM and TEM images also clearly confirmed that no metal catalyst droplets were found at the tips of the nanowires.

The source of the oxygen in this procedure may be attributed to the SiO_2 layer on the surface of the Si substrate and the surviving oxygen (O_2 and H_2O) in the refractory inside the furnace. The mullite refractory lining may also result in a rise in oxygen content at high temperatures [25,26]. Therefore, the surviving oxygen will directly react with the graphite powder to yield CO vapor according to the following reaction:

$$C(s)+O_2(g)\rightarrow 2CO(g) \quad (1)$$

When the temperature rose gradually, the graphite powder was vaporized to form the C vapor [27]. Then SiO vapor was generated by the reaction of the SiO_2 layer on the surface of the Si substrate with C vapor according to the following reactions:

$$SiO_2(s)+C(g)\rightarrow SiO(g)+CO(g) \quad (2)$$

$$SiO_2(s)+CO(g)\rightarrow SiO(g)+CO_2(g) \quad (3)$$

Besides, at temperatures above 1000 °C, the SiO vapor could also be produced by the reaction of the SiO_2 layer with the Si substrate [23,28]:

$$Si(s)+SiO_2(s)\rightarrow 2SiO(g) \quad (4)$$

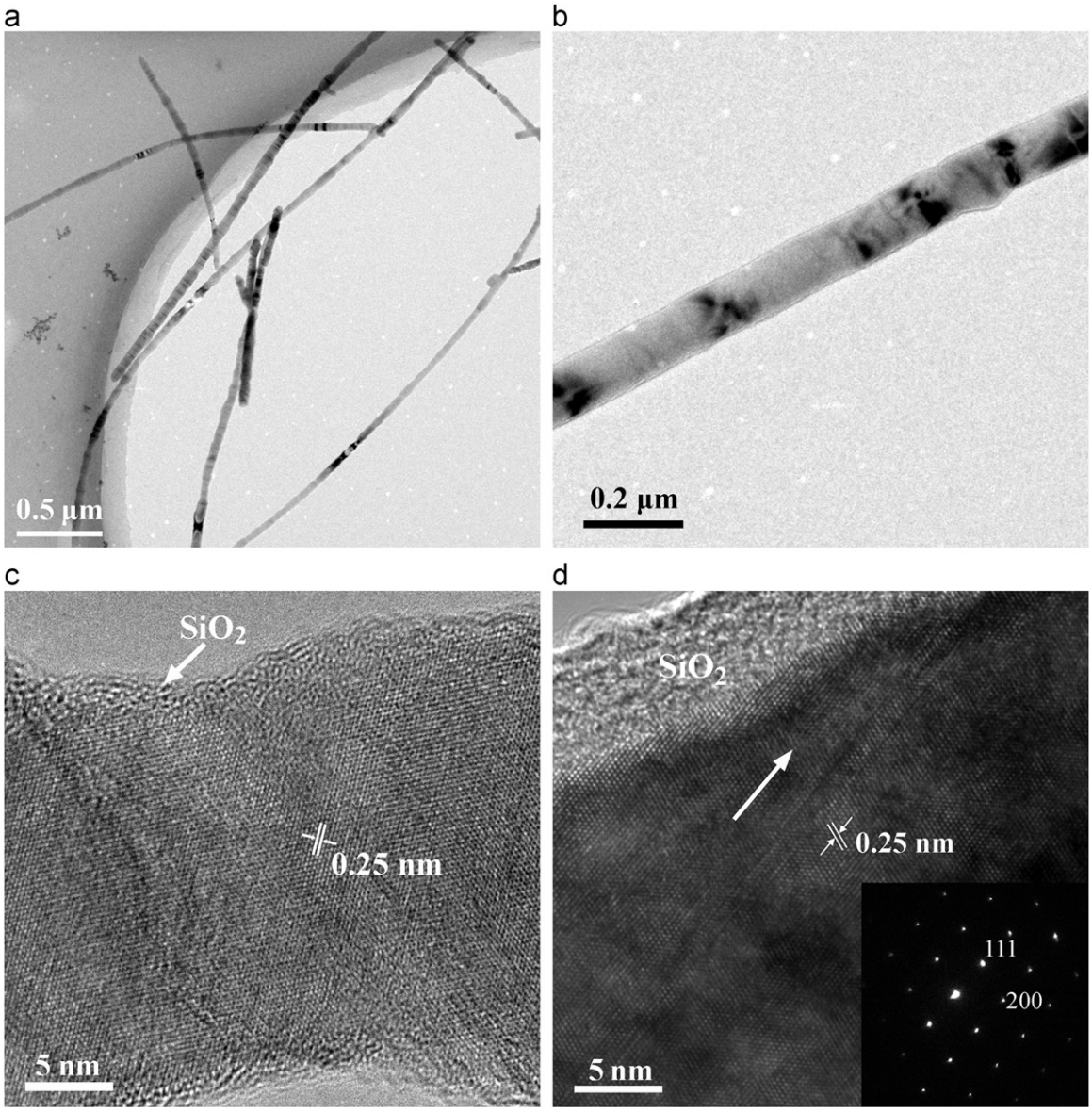

Fig. 4. (a) and (b) Typical low and high magnification TEM images of SiC nanowires, respectively. (c) and (d) HRTEM images of SiC nanowires. The inset in (d) is the corresponding SAED pattern of the SiC core.

Subsequently, the SiO vapor formed in the above-mentioned reactions reacted further with the solid graphite and CO in accordance with reactions (5) and (6). Additionally, it is well known that the CO_2 vapor generated will be reduced by the carbon source to yield CO vapor (reaction (7)):

$$SiO(g)+2C(s)\rightarrow SiC(s)+CO(g) \quad (5)$$

$$SiO(g)+3CO(g)\rightarrow SiC(s)+2CO_2(g) \quad (6)$$

$$CO_2(g)+C(s)\rightarrow 2CO(g) \quad (7)$$

SiC crystal nuclei were generated by the above vapor–solid reactions (Fig. 5(a)). It is believed that SiC crystal nuclei are apt to be formed at the most active positions of the defects or impurities on the Si substrate [20]. Afterwards, the formed SiC nuclei acted as seeding and interconnected to form SiC nanowires along the preferential crystalline direction, namely the (111) plane because of reasons based upon the lowest-energy principle (as shown in Fig. 5(b) and (c)). The EDS results of area 1 in Fig. 5(a) and area 2 in Fig. 5(b) are given in Fig. 5(d) and (e), respectively, where it can be seen that the atomic percentages of Si increased slightly in the growth process of the SiC nanowires.

Here one case should be mentioned, as the CO vapor further diffused to the surface of the Si substrate, the Si substrate reacted directly with the gaseous phase carbon and generated SiC nanowires :

$$Si(s)+2CO(g)\rightarrow SiC(s)+CO_2 \quad (8)$$

It is noted that the synthesized SiC nanowires had a SiC–SiO_2 core–shell structure. Previous investigations have

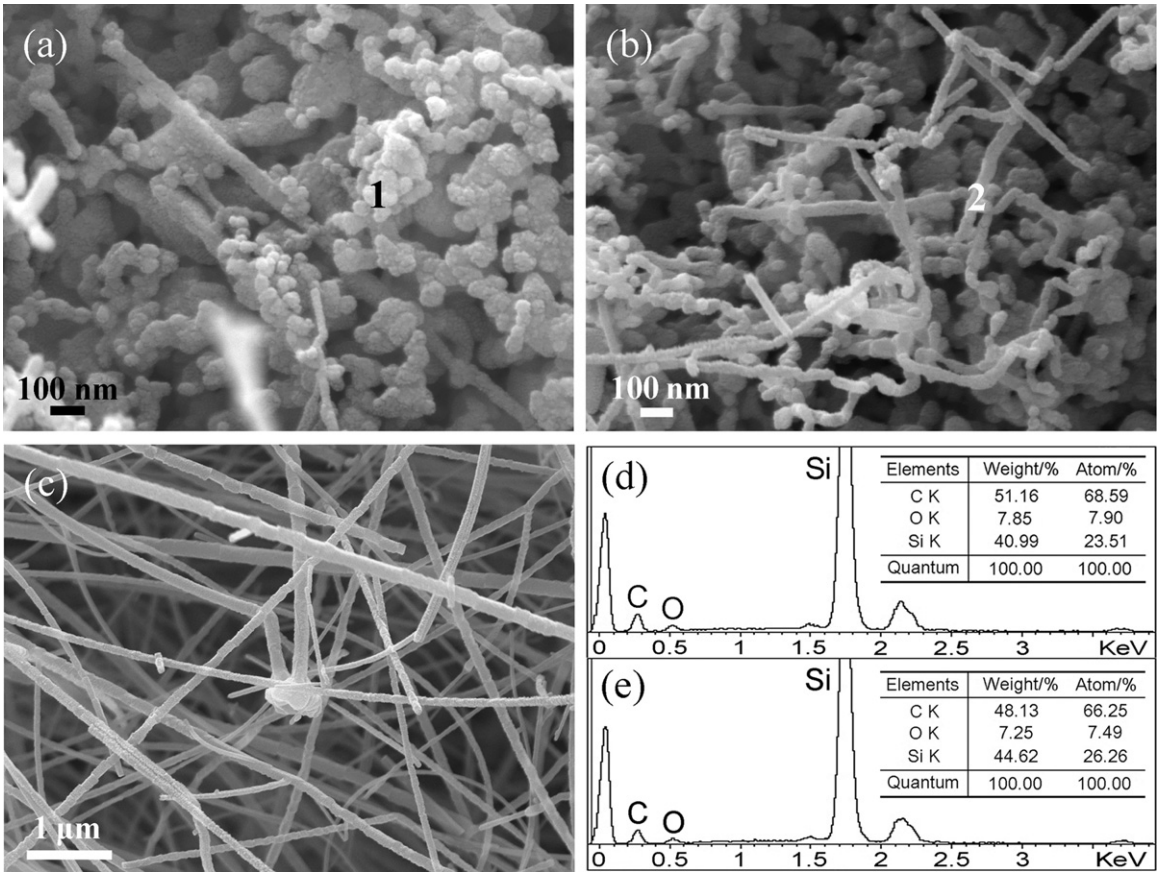

Fig. 5. (a) Typical FESEM image of SiC crystal nuclei. (b) and (c) FESEM images of SiC nanowires. (d) and (e) EDS patterns of area 1 in (a) and area 2 in (b), respectively.

revealed that the solidification of the SiC core happens faster than that of the viscous SiO_2 layer because of the melting point of SiC, which is much higher than that of SiO_2 [14,29,30]. For this reason, a thin amorphous SiO_2 layer will be formed and wraps the crystalline SiC nanowires during the cooling procedure. As mentioned above, the following reactions will occur:

$$2SiO(g)+C(g)\rightarrow SiC(s)+SiO_2(s) \quad (9)$$

$$3SiO(g)+CO(g)\rightarrow SiC(s)+2SiO_2(s) \quad (10)$$

4. Conclusions

In summary, scales of SiC nanowires were successfully synthesized on Si (100) wafer by the thermal evaporation method without the assistance of a metal catalyst. The as-obtained SiC nanowires grew along the [111] direction and possessed diameters of 50–100 nm and lengths of several hundreds of microns. The SiC nanowire was composed of a single-crystalline SiC core with a thin amorphous SiO_2 shell. On the basis of the experimental results, the growth mechanism of SiC nanowires was considered to involve a vapor–solid process.

Acknowledgment

The authors greatly appreciate the National Natural Science Foundation of China (Grant nos. 51032007 and 50972134), the Fundamental Research Funds for the Central Universities (Grant no. 2010ZD12), and the New Star Technology Plan of Beijing (Grant no. 2007A080) for financial support. K. Chen especially thanks Mr. Bingyang Wu for providing the Si wafer applied in this work.

References

[1] Z.L. Wang, Z.R. Dai, Z.G. Bai, R.P. Gao, J.L. Gole, Side-by-side silicon carbide–silica biaxial nanowires: synthesis, structure and mechanical properties, Applied Physics Letters 77 (2000) 3349–3351.
[2] Z.W. Pan, Z.R. Dai, Z.L. Wang, Nanobelts of semiconducting oxides, Science 291 (2001) 1947–1949.
[3] Z.L. Wang, J.H. Song, Piezoelectric nanogenerators based on zinc oxide nanowire arrays, Science 312 (2006) 242–246.
[4] Y.N. Xia, P.D. Yang, Y.G. Sun, Y.Y. Wu, B. Mayers, B. Gates, Y.D. Yin, F. Kim, H.Q. Yan, One-dimensional nanostructures: synthesis, characterization, and applications, Advanced Materials 15 (2003) 353–389.
[5] C.M. Lieber, Nanowire superlattices, Nano Letters 2 (2002) 81–82.
[6] Z.W. Pan, H.L. Lai, Frederick C.K. Au, X.F. Duan, W.Y. Zhou, W.S. Shi, N. Wang, C.S. Lee, N.B. Wong, S.T. Lee, S.S. Xie, Oriented silicon carbide nanowires: synthesis and field emssion properties, Advanced Materials 12 (2000) 1186–1190.

[7] W.M. Zhou, L.J. Yan, Y. Wang, Y.F. Zhang, SiC nanowires: a photocatalytic nanomaterial, Applied Physics Letters 89 (2006) 13105–13107.
[8] J. Wei, K.Z. Li, H.J. Li, Q.G. Fu, L. Zhang, Growth and morphology of one-dimensional SiC nanostructures without catalyst assistant, Materials Chemistry and Physics 95 (2006) 140–144.
[9] G. Gundiah, G.V. Madhav, A. Govindaraj, M.M. Seikh, C.N.R. Rao, Synthesis and characterization of silicon carbide, silicon oxynitride and silicon nitride nanowires, Journal of Materials Chemistry 12 (2002) 1606–1611.
[10] H. Ye, N. Titchenal, Y. Gogotsi, F. Ko, SiC nanowires synthesized from electrospun nanofiber templates, Advanced Materials 17 (2005) 1531–1535.
[11] W.Q. Han, S.S. Fan, Q.Q. Li, B.L. Gu, D.P. Yu, Continuous synthesis and characterization of silicon carbide nanorods, Chemical Physics Letters 265 (1997) 374–378.
[12] R.B. Wu, G.Y. Yang, Y. Pan, J.J. Chen, Synthesis of silicon carbide hexagonal nanoprisms, Applied Physics A 86 (2007) 271–274.
[13] J.J. Niu, J.N. Wang, An approach to the synthesis of silicon carbide nanowires by simple thermal evaporation of ferrocene onto silicon wafers, European Journal of Inorganic Chemistry 2007 (2007) 4006–4010.
[14] K. Senthil, K. Yong, Enhanced field emission from density-controlled SiC nanowires, Materials Chemistry and Physics 112 (2008) 88–93.
[15] Z.J. Li, H.J. Li, X.L. Chen, A.L. Meng, K.Z. Li, Y.P. Xu, L. Dai, Large-scale synthesis of crystalline β-SiC nanowires, Applied Physics A 76 (2003) 637–640.
[16] Q.G. Fu, H.J. Li, X.H. Shi, K.Z. Li, J. Wei, Z.B. Hu, Synthesis of silicon carbide nanowires by CVD without using a metallic catalyst, Materials Chemistry and Physics 100 (2006) 108–111.
[17] W.M. Zhou, B. Yang, Z.X. Yang, F. Zhu, L.J. Yan, Y.F. Zhang, Large-scale synthesis and characterization of SiC nanowires by high-frequency induction heating, Applied Surface Science 252 (2006) 5143–5148.
[18] W.Y. Yang, H.Z. Miao, Z.P. Xie, L.G. Zhang, L.N. An, Synthesis of silicon carbide nanorods by catalyst-assisted pyrolysis of polymeric precursor, Chemical Physics Letters 383 (2004) 441–444.
[19] H. Huang, J.T. Fox, F.S. Cannon, S. Komarneni, In situ growth of silicon carbide nanowires from anthracite surfaces, Ceramics International 37 (2011) 1063–1072.
[20] R.B. Wu, G.Y. Yang, Y. Pan, L.L. Wu, J.J. Chen, M.X. Gao, R. Zhai, J. Lin, Thermal evaporation and solution strategies to novel nanoarchitectures of silicon carbide, Applied Physics A 88 (2007) 679–685.
[21] E.L. Zhang, Y.H. Tang, Y. Zhang, C. Guo, Synthesis and photoluminescence property of silicon carbon nanowires synthesized by the thermal evaporation method, Physica E 41 (2009) 655–659.
[22] P.C. Kang, B. Zhang, G.H. Wu, J. Su, H.S. Gou, Synthesis of SiO_2 covered SiC nanowires with milled Si,C nanopowders, Materials Letters 65 (2011) 3461–3464.
[23] W. Khongwong, K. Yoshida, T. Yano, Simple approach to fabricate SiC–SiO_2 composite nanowires and their oxidation resistance, Materials Science and Engineering: B 173 (2010) 117–121.
[24] I. Berman, C.E. Ryan, The growth of silicon carbide needles by the vapor–liquid–solid method, Journal of Crystal Growth 9 (1971) 314–318.
[25] W. Khongwong, M. Imai, K. Yoshida, T. Yano, Synthesis of β-SiC/SiO_2 core–shell nanowires by simple thermal evaporation, Journal of the Ceramic Society of Japan 117 (2009) 194–197.
[26] J.J. Niu, J.N. Wang, A simple route to synthesize scales of aligned single-crystalline SiC nanowires arrays with very small diameter and optical properties, Journal of Physical Chemistry B 111 (2007) 4368–4373.
[27] L.M. Ghiringhelli, C. Valeriani, J.H. Los, E.J. Meijer, A. Fasolino, D. Frenkel, State-of-the-art models for the phase diagram of carbon and diamond nucleation, Molecular Physics 106 (2008) 2011–2038.
[28] B.H. Djamila, P. Perrot, Thermodynamics of the Au–Si–O System: application to the synthesis and growth of silicon-silicon dioxide nanowires, Journal of Phase Equilibria and Diffusion 28 (2007) 150–157.
[29] B. Park, Y. Ryu, K. Yong, Growth and characterization of silicon carbide nanowires, Surface Review and Letters 11 (2004) 373–378.
[30] S.Z. Deng, Z.B. Li, W.L. Wang, N.S. Xu, Z. Jun, X.G. Zheng, H.T. Xu, C. Jun, J.C. She, Field emission study of SiC nanowires/nanorods directly grown on SiC ceramic substrate, Applied Physics Letters 89 (2006) 23118–23120.